Dynamical simulations of two density-coupled 1D Bose-Einstein condensates

Author: Sandra Coll-Vinent Wappenhans.
Facultat de Física, Universitat de Barcelona, Diagonal 645, 08028 Barcelona, Spain.

Advisor: Bruno Julià Díaz
(Dated: June 12, 2019)

Abstract: We consider a system of two trapped density-coupled Bose-Einstein condensates in 1D, described by the coupled Gross-Pitaevskii equations. We perform numerical simulations to study the stability of two stationary states: the ground state and a dark-antidark soliton state. By perturbing these states we characterize their oscillation frequency and find that it decreases for increasing interspecies interaction. Our numerical results are in agreement with analytical predictions found in the literature.

I. INTRODUCTION

Bose-Einstein condensates (BECs) spark great interest because they allow for the observation of quantum physics on the macroscopic scale. This phenomenon is related to several branches of physics such as superfluidity, superconductivity, lasers, nonlinear optics, and physics of nonlinear waves [1]. The BEC was predicted by S.N. Bose and A. Einstein in 1924 [2], and it was only after 70 years that a BEC was experimentally observed in trapped atomic clouds [3]. Since then, a large amount of both theoretical and experimental studies have been realised [4].

Nowadays, it is possible to cool down and trap atoms by use of electromagnetic fields. This allows for a very precise tuning of the physical properties of BECs [5]. Low dimensional BECs have been experimentally realised in atom traps, such as cigar-shaped 1D condensates and disk-shaped 2D condensates [6]. Mixtures of BECs have also been obtained [7], using two hyperfine states or two atomic species. This recently acquired control over the characteristics of the BEC, motivates its further studying in different configurations. In particular, a 1D two-component configuration that will be analysed in this study.

This present work consists on the analysis of two density-coupled BECs in 1D described by the coupled Gross-Pitaevskii (GP) equations. Specifically, the stability of the ground state (GS), and the excited dark-antidark state will be studied.

This study is organised as follows. In Section II, the theoretical framework of the system under study is described. In Section III we expose and test the numerical algorithms used to solve the GP equations. In section IV the two analysed configurations are defined and results of the simulations are presented. In Section V, conclusions are drawn.

II. SYSTEM DESCRIPTION

A. Single component condensate

At zero temperature, a one-dimensional Bose-Einstein condensate can be described in the mean-field approximation by the Gross-Pitaevskii equation,

$$i\hbar\frac{\partial\overline{\psi}}{\partial\bar{t}} = \left[-\frac{\hbar^2}{2m}\partial_{\bar{x}}^2 + \overline{V}(\bar{x}) + \bar{g}|\overline{\psi}|^2\right]\overline{\psi}, \tag{1}$$

where $\overline{\psi}_1$ is the wave function normalized to 1 and $\overline{V}(\bar{x})$ is an arbitrary trapping potential. The interaction between the bosons is represented by a contact delta potential, with strength g. The time-independent GP equation is then

$$\left[-\frac{\hbar^2}{2m}\partial_{\bar{x}}^2 + \overline{V}(\bar{x}) + \bar{g}|\overline{\psi}|^2\right]\overline{\psi} = \bar{\mu}\overline{\psi}. \tag{2}$$

Where $\bar{\mu}$ corresponds to the chemical potential.

If we consider a harmonic potential trap $\overline{V}(\bar{x}) = m\omega^2\bar{x}^2/2$, it is convenient to rewrite the equations using the harmonic oscillator units: $t = \bar{t}/t_{ho}$, $E = \overline{E}/e_{ho}$, $x = \bar{x}/a_{ho}$, $g = \bar{g}/e_{ho}a_{ho}$ and $\mu = \bar{\mu}/e_{ho}$, where $t_{ho} = \omega^{-1}$, $e_{ho} = \hbar\omega$ and $a_{ho} = \sqrt{\hbar/m\omega}$. In these units, Eq. (1) reduces to,

$$i\frac{\partial\psi}{\partial t} = \left[-\frac{1}{2}\partial_x^2 + \frac{1}{2}x^2 + g|\psi|^2\right]\psi, \tag{3}$$

and Eq. (2), to:

$$\left[-\frac{1}{2}\partial_x^2 + \frac{1}{2}x^2 + g|\psi|^2\right]\psi = \mu\psi. \tag{4}$$

When the interaction term is much larger than the kinetic energy term, that is for large g, we can neglect the latter. This is known as the *Thomas-Fermi approximation*, in which Eq. (4) becomes:

$$\left[\frac{1}{2}x^2 + g|\psi|^2\right]\psi = \mu\psi. \tag{5}$$

Eq. (5) can be solved analytically and yields the following wave function,

$$\psi_{\mathrm{TF}}(x) = \begin{cases}\sqrt{\mu - \frac{1}{2}x^2} & |x| < \sqrt{2\mu}\\ 0 & |x| > \sqrt{2\mu},\end{cases} \tag{6}$$

called the *Thomas-Fermi solution* (TF). Where $\mu = \left(3g/4\sqrt{2}\right)^{2/3}$ is found by normalization.

In the framework of an untrapped BEC, i.e. $\overline{V}(\bar{x}) = 0$, there is an analytical solution for Eq. (2) with the form

$$\overline{\psi}_{DS}(\bar{x}) = \sqrt{n_0}\tanh\left(\bar{x}/\bar{\xi}\right), \tag{7}$$

where n_0 is the background density [8]. This stationary solution is called a *dark soliton*. It has been long-known by nonlinear optics and it receives that name because it describes a dark spot in a light pulse [9]. The quantity $\bar{\xi} = \hbar/\sqrt{m\bar{g}n_0}$ is known as the healing length and it is a measure of the length scale of the soliton [10].

B. Two density-coupled components

In our study, we will consider two density-coupled BECs in a harmonic potential trap. Therefore from now on all the expressions will be written in harmonic oscillator units.
Two density-coupled BECs are well described by the following coupled GP equations:

$$\begin{aligned} i\frac{\partial\psi_1}{\partial t} &= \left[-\frac{1}{2}\partial_x^2 + \frac{1}{2}x^2 + g_{11}|\psi_1|^2 + g_{12}|\psi_2|^2\right]\psi_1 \\ i\frac{\partial\psi_2}{\partial t} &= \left[-\frac{1}{2}\partial_x^2 + \frac{1}{2}x^2 + g_{22}|\psi_2|^2 + g_{12}|\psi_1|^2\right]\psi_2, \end{aligned} \tag{8}$$

where ψ_1 and ψ_2 are the wave functions that describe each component. g_{11}, g_{22} and g_{12} represent the interaction strength between bosons of the first component, second component and the cross interaction between them, respectively. These equations can be pictured as a set of nonlinear Schrödinger equations. The expressions in brackets can be understood as an effective hamiltonian, where $-\partial_x^2/2$ is the kinetic energy term and the rest can be viewed as an effective potential.

III. NUMERICAL METHODS

A. Solution of the GP equation

The aim of this work is to study the dynamical stability of two density-coupled BECs for different configurations. For that purpose, we have numerically solved Eq. (8). First we have obtained a stationary state of the equation, and after that, we have perturbed it to study its dynamical stability.
To achieve a stationary state of Eq. (8) we have used the *imaginary time* method. For section IV A, this method has been used to obtain the GS. And for section IV B it has been used to produce an excited state with a displaced soliton in one component, known as a *dark-antidark soliton*, which will be discussed further below.
Interestingly enough, we have found that the *imaginary time* method can yield a quasi-stationary state with a displaced soliton. That is achieved when we start the one component *imaginary time* method with

$$\psi^0_{\rm sol}(x,d) = \psi_{\rm TF}(x)\tanh\left(x-d\right), \tag{9}$$

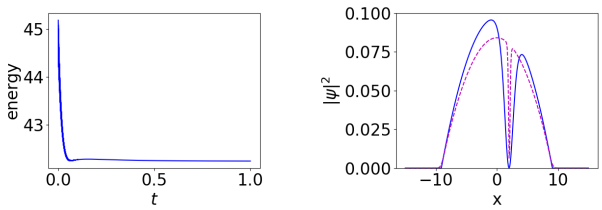

FIG. 1. On the left panel, energy convergence of the imaginary time evolution of $\psi^0_{sol}(x,2)$. On the right panel, initial density profile corresponding to the wave function $\psi^0_{sol}(x,2)$ (solid blue line), and profile density corresponding to the state evolved in imaginary time for 1 t_{ho} (dashed magenta line).

where the hyperbolic tangent adds a zero in the density profile at d. When we let this state evolve in imaginary time, we see that its energy quickly converges and stays in a quasi-stable plateau, as shown in Fig. 1. The state resulting after the energy convergence is a quasi-stationary state with a displaced soliton, also shown in Fig. 1.
For section IV A, after having obtained the desired initial state through the imaginary time method, we proceed to perturb it and evolve it in real time. For section IV B, the imaginary time evolution already provides us with a perturbed quasi-stationary state (a soliton displaced from the center in one component), so we directly proceed to evolve it in real time.

B. Numerical solver

In both cases, imaginary and real time evolution, we solve Eq. (8) using the *Crank-Nicolson* method. This method is a finite difference method used to solve partial differential equations, which considers the spatial second derivative as the mean of its calculation in two consecutive time-steps. A tridiagonal system of algebraic equations must be solved at every time-step, and for that purpose we use the *tridiagonal matrix algorithm* [11]. As the effective hamiltonian contains $|\psi_1(t)|$ and $|\psi_2(t)|$, we use their values from the previous time step at every iteration, starting with the given initial states. The method has been shown to be stable for $r = dt/dx^2 \leq 1/2$ for the heat equation [12], but for our equations it gave instabilities as far as for $r = 0.1$, so for all our calculations we used $r = 0.01$, which proved to be stable. The discretization used for this present work has been $dx = 0.1$ and $dt = 0.0001$ in a box of length $L = 15$ with $g_{11} = g_{22} = 500$. In what follows, we will use $g_{11} = g_{22} = g$.

C. Numerical tests in a single component case

We have tested both the imaginary time and the real time program to work under some known conditions. For example, if we set $g = 0$ in Eq. (3), we recover the Schrödinger equation with a harmonic potential. For

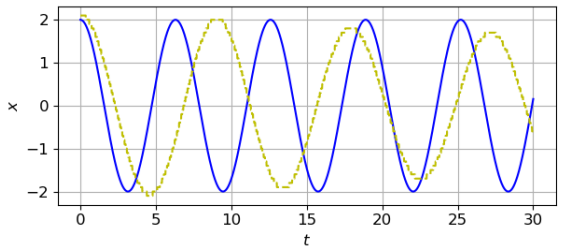

FIG. 2. The solid blue line shows the numerical results for the time evolution of the mean position of the GS in one component (with frequency $\nu_{GS} = 0.1578$). The dashed yellow line shows the soliton minimum time evolution in one component (with frequency $\nu_{\rm sol} = 0.1109$).

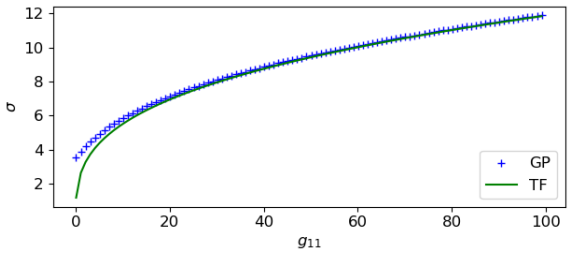

FIG. 3. $\sqrt{\langle x^2\rangle - \langle x\rangle^2}$ is shown in function of g_{11} for the GS of Eq. (3) (blue crosses) and for $\psi_{TF}(x)$ (solid green line).

that case, the *imaginary time* method has been tested to return the harmonic oscillator (HO) GS when starting from a wider initial Gaussian wave function. And to return the first HO excited state when starting from a state orthogonal to the GS. When evolving the obtained GS in real time, it has been tested to remain stationary, and when displaced from the centre it has been tested to oscillate at a frequency $\nu = 0.158 \approx 1/2\pi = \nu_{\rm trap}$ (shown in Fig. 2).

Setting again $g = 500$, and starting the imaginary time from $\psi^0_{\rm sol}(x, 2)$, we obtain an off-centered soliton in one component. Then we evolve this quasi-stationary state in real time and see that the soliton minimum oscillates with a frequency $\nu_{sol} = 0.111 \approx \nu_{\rm trap}/\sqrt{2}$, (also shown in Fig. 2). This soliton oscillation frequency in the trapped case is well known for the TF limit [13].

We have also checked that the GS of the GP equation approaches the TF solution as g is increased. For that, we have obtained the GS of Eq. (3) through the imaginary time method for a range of g. In Fig. 3, the size of the atomic cloud of the GS, measured by $\sqrt{\langle x^2\rangle - \langle x\rangle^2}$, is compared with the analytical prediction for the TF. It shows indeed an excellent agreement for large g.

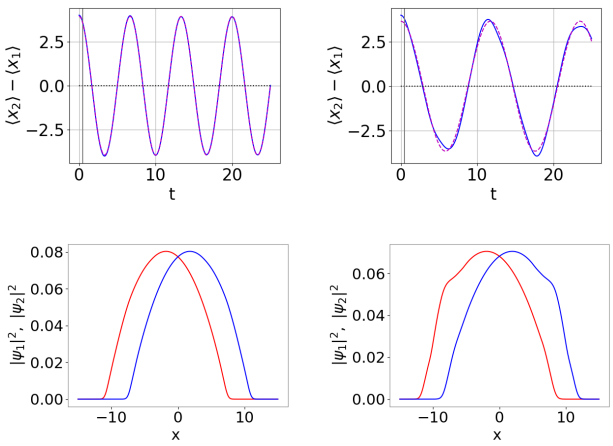

FIG. 4. The upper panels show the time evolution of the relative mean position of each component (solid blue line), a sine-wave fit (dashed magenta line) and the position of the center of mass of the system (dotted black line). The lower panels show $|\psi_1(x, t = 0.5)|^2$ and $|\psi_2(x, t = 0.5)|^2$, i.e. the density profile of the states at the time signaled with a vertical gray line in the upper panels. In the left panels $g_{12}/g = 0.08$ and in the right panels $g_{12}/g = 0.6$.

IV. DYNAMICAL SIMULATIONS

The aim of this section is to analyse the dynamics of two interacting components when varying the interspecies interaction g_{12}.

A. Out of phase mode of the GS

In this subsection we are interested in studying the dynamical stability of the GS. In particular, we want to excite the out of phase mode by symmetrically displacing each component from their equilibrium position, without displacing the center of mass of the system. The aim is to characterize the relative oscillation frequency of the two components for a range of g_{12}/g from 0 to 1. We expect to find for $g_{12}/g = 0$ a frequency $\nu_{\rm rel} = 1/2\pi$, i.e. the frequency of the trap, and no oscillation ($\nu_{\rm rel} = 0$) for $g_{12}/g = 1$, as the two components will be immiscible. To obtain the GS of the system under study we have evolved the states $\psi^0_1(x)$, $\psi^0_2(x) = \psi_{\rm TF}(x)$ in imaginary time, for a certain g_{12}/g. The resulting state of that simulation, i.e. the GS, is a centered TF-like density profile in each component, widdened by the interspecies interaction. To excite the out of phase mode, we have displaced each component a distance 2 from the center in opposite directions. Subsequently, we have evolved the perturbed GS in real time. The upper panels in Fig. 4 show the evolution of the relative position of the mean of each component in time for two different g_{12}/g. They also show that the center of mass of the system remains still, so we have indeed excited the out of phase mode. We see that the two components oscillate, so we verify

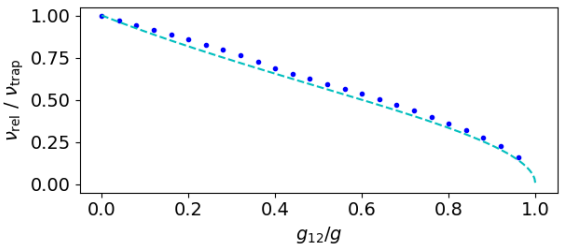

FIG. 5. Numerical results for the dependence of the relative oscillation frequency on g_{12}/g (blue dots) compared to the analytical prediction of Eq.10 (cyan dashed line).

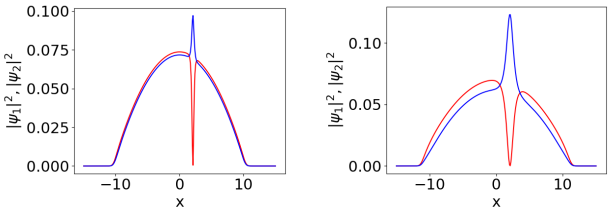

FIG. 6. Dark-antidark soliton density profile, displaced a distance 2 from the center. In the left panel, $g_{12}/g = 0.48$ and in the right panel $g_{12}/g = 0.96$.

the stability of the GS. To obtain the main frequency of that relative oscillations we have fit a sine wave to the relative mean position data, as depicted in the figure.
We can see that other oscillation frequencies appear for the higher interspecies interaction, as the data is slightly deviated from the sine fit. The density profile of each component is deformed from its initial state as it evolves in time, as expected, for the system is no longer in its GS. As the relative interaction increases, the density profiles of each component suffer during the evolution a larger symmetric deformation from their initial TF-like shape. This can be seen in the lower panels of Fig. 4, where for lower relative interaction the states are less deformed than for higher relative interactions, where we can see bumps growing on the sides due to the mutual repulsion of the approaching components. It is these symmetric deformations that lead to the appearance of other frequencies. In any case, we will only consider the main frequency obtained through the sine fit, for all g_{12}/g.
We can now study the dependence of the relative oscillation frequency on g_{12}/g (Fig. 5). For that purpose we have run the previously described simulations for g_{12}/g from 0 to 1 every 0.04, with a duration of 25 t_{ho} each. As we expected, $\nu_{\text{rel}}(g_{12}/g = 0) = 0.159 \approx \nu_{\text{trap}}$ and $\nu_{\text{rel}}(g_{12}/g = 1) = 0$. We see that for greater g_{12}/g the relative oscillation frequency decreases. This decrease is due to the increasing repulsion that each component has to overcome to cross over the other.
In reference [14] they provide the following prediction for the studied oscillation mode of the GS:

$$\nu_{\text{rel}}/\nu_{\text{trap}} = \sqrt{\frac{1 - g_{12}/g}{1 + g_{12}/g}}. \tag{10}$$

In Fig. 5 we compare our numerical results with that prediction and find a reasonable agreement.

B. Dark-Antidark soliton

A dark-antidark soliton is a two-component configuration that arises from the interaction between a dark soliton in one component and a TF-like state in the other. The absence of particles in the soliton attracts particles from the other component, due to the lack of coupling repulsion. Therefore, particles from the second component will build up in the soliton dip, forming what is known as a dark-antidark soliton [14].
In what follows, we are going to focus on studying the stability of the dark-antidark soliton when displaced from its equilibrium position. In particular, we want to characterize how the oscillation of a dark-antidark soliton on a TF-like background depends on g_{12}/g. We expect that for $g_{12}/g = 0$, we will obtain a regular gray soliton in one component, oscillating with $\nu = \nu_{\text{trap}}/\sqrt{2}$. The dark-antidark soliton configuration can only exist for $g_{12}/g \leq 1$, as for $g_{12}/g = 1$ we reach the miscibility-immiscibility threshold, in which both components cannot coexist. For $g_{12}/g = 1$ we expect the system to be stationary ($\nu = 0$) with a summed density profile of $|\psi_1(x)|^2 + |\psi_2(x)|^2 = |\psi_{\text{TF}}(x)|^2$. This limiting system can be thought of as a one component system (as $g = g_{22} = g_{12}$) which consequently has a TF as a total density profile for the GS.
The off-centered dark-antidark soliton state is achieved by letting evolve in imaginary time the initial states $\psi_1^0(x) = \psi_{\text{sol}}^0(x, 2)$ and $\psi_2^0(x) = \psi_{\text{TF}}(x)$ for a certain g_{12}/g. The initial state of the first component will yield a displaced soliton profile after the imaginary time evolution. The second component will see an attractive potential well in the position of the soliton and will develop a bump there, resulting in the off-centered *dark - antidark* soliton shown in Fig. 6. As we increase the interaction, more matter is accumulated inside the soliton and the wider the soliton becomes, as can be seen comparing the two panels in Fig. 6.

To study how the oscillation of the *dark - antidark soliton* depends on g_{12}/g, we obtain the described initial states for a range of g_{12}/g from 0 to 1 every 0.04. Subsequently, we evolve each state in real time for 10 t_{ho}. We verify that the dark and anti-dark solitary waves oscillate together through the background (the system is therefore stable) without being deformed. Similarly to the previous section, we fit a sine-wave to the minimum position of the soliton to get the oscillation frequency of the *dark-antidark soliton*. The sine-wave was well fitted for all g_{12}/g.
Fig. 7 shows the oscillation frequencies of the *dark-antidark soliton* for the studied range of g_{12}/g. We

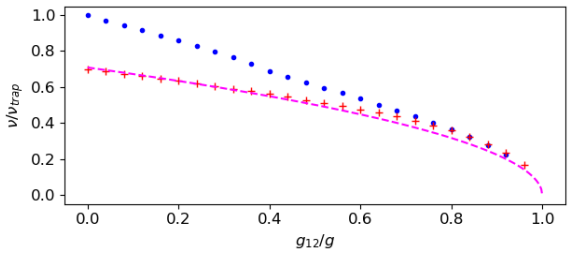

FIG. 7. Dependence of the oscillation frequency of the dark-antidark soliton on g_{12}/g (red crosses) and the analytical prediction from Eq. (11) (magenta dashed line). Also compared with the out of phase oscillation frequency of the GS from Fig. 5 (blue dots).

have checked that for $g_{12}/g = 0$ the frequency is indeed $\nu = 0.111 \approx \nu_{\text{trap}}/\sqrt{2}$ and that it tends to 0 for $g_{12}/g = 1$. We can see that the frequency of oscillation decreases for increasing g_{12}/g, which is the behaviour that we would expect in between the limiting configurations stated above. Solitons can usually be described as quasiparticles [15]. The frequency decrease can be viewed as a consequence of the increasing repulsive interaction of the quasiparticle with its surroundings, which slows down its movement.
We also compare our figure with a theoretical prediction from [14]:

$$\nu/\nu_{\text{trap}} = \sqrt{\frac{1 - g_{12}/g}{2}}. \tag{11}$$

A reasonably similar behaviour is found with our corresponding numerical result.

It is also interesting to compare the relative oscillation frequencies of the GS from the previous section with the ones of the dark-antidark soliton. We can see in Fig. 7 that both frequencies merge near $g_{12}/g = 0.8$. This convergence can also be inferred from Eqs. 10 and 11 when $g_{12}/g \to 1$. In Ref. [14], they also find this resonance between the two oscillation modes.

V. CONCLUSIONS

We have studied the dynamics of two trapped density-coupled BECs in 1D described by the mean-field theory GP equations. In particular, the stability of the GS and of an excited state known as a dark anti-dark soliton has been analysed for different interspecies interactions. We have shown that both states are stable (they oscillate) under off-center perturbations, for $g_{12}/g < 1$. Their oscillation frequencies have been found to decrease for increasing interspecies interaction. This behaviour has been intuitively explained as the result of an increasing difficulty for the two components to overcome mutual repulsive interaction. Our numerical simulations have been shown to be in good agreement with the analytical predictions from Ref. [14].
Regarding the technical aspects of this work, we have found that the imaginary time method, a part from giving stationary states of the GP equations, is also able to yield a quasi-stationary displaced dark-antidark soliton. Furthermore, we have verified that the Crank-Nicolson method is useful to numerically evolve states in the GP equations both in imaginary and real time.

VI. ACKNOWLEDGEMENTS

I would like to express my gratitude to Bruno Julià, Iván Morera and Artur Polls for their guidance and support in developping this project.

[1] D. Frantzeskakis, J. Phys. A **43**, 213001 (2010).
[2] S. Bose, "Plancks gesetz und lichtquantenhypothese," Zeitschrift für Physik (1924).
[3] M. H. Anderson, J. R. Ensher, M. R. Matthews, C. E. Wieman, and E. A. Cornell, Science **269**, 198 (1995).
[4] L. Pitaevskii and S. Stringari, "Bose-einstein condensation," Oxford University Press (2003).
[5] J. I. Cirac and P. Zoller, Science **301**, 176 (2003).
[6] A. Görlitz, J. Vogels, A. Leanhardt, C. Raman, T. Gustavson, J. Abo-Shaeer, A. Chikkatur, S. Gupta, S. Inouye, T. Rosenband, *et al.*, Phys. Rev. Lett. **87**, 130402 (2001).
[7] C. J. Myatt, E. A. Burt, R. W. Ghrist, E. A. Cornell, and C. E. Wieman, Phys. Rev. Lett. **78**, 586 (1997).
[8] L. L. Olivella, (Bachelor Thesis) Universitat de Barcelona (2019).
[9] T. Busch and J. R. Anglin, Phys. Rev. Lett. **84**, 2298 (2000).
[10] L. D. Carr, J. Brand, S. Burger, and A. Sanpera, Phys. Rev. A **63**, 051601 (2001).
[11] L. H. Thomas, Watson Sci. Comput. Lab. Rept., Columbia University, New York **1** (1949).
[12] C. M. Oishi, J. Y. Yuan, J. A. Cuminato, and D. E. Stewart, BIT Numer. Math. **55**, 487 (2015).
[13] V. V. Konotop and L. Pitaevskii, Phys. Rev. Lett. **93**, 240403 (2004).
[14] I. Danaila, M. Khamehchi, V. Gokhroo, P. Engels, and P. Kevrekidis, Phys. Rev. A **94**, 053617 (2016).
[15] C. Qu, L. P. Pitaevskii, and S. Stringari, Phys. Rev. Lett. **116**, 160402 (2016).